

BIOCHE 01652

Dissociation of *Limulus polyphemus* (Horseshoe Crab) Hemocyanin. II. Stopped-flow X-ray scattering study

Kazumoto Kimura ^a, Yoshihiko Igarashi ^b, Hirotsugu Tsuruta ^c, Hiroshi Kihara ^d and Akihiko Kajita ^b

^a Division of Medical Electronics, and ^b Department of Biochemistry, Dokkyo University School of Medicine, Mibu, Tochigi 321-02 (Japan)

^c Department of Materials Science, Faculty of Science, Hiroshima University, Hiroshima 730 (Japan)

^d Jichi Medical School, School of Nursing, Minamikawachi, Tochigi 329-04 (Japan)

(Received 13 November 1991; accepted in revised form 30 November 1991)

Abstract

Dissociation kinetics of *Limulus polyphemus* hemocyanin, induced by calcium removal was studied by the stopped-flow X-ray scattering (SFXS) method and fluorescence stopped-flow method at various pH. Between pH 6.3 and 8.4, the time course of the kinetics showed a lag followed by a single exponential decay, while it obeyed a single exponential decay without a lag at pH 8.8. To analyze the process, equations to calculate zero angle intensity, I_0 , and radius of gyration, R_g , were presented. Simulated curves from the equations fitted the data well. Concerning either of I_0 and R_g , the lag-time decreased with increasing EDTA concentration, while the apparent rate constant of the dissociation, k_{app} , increased. Based on the value of I_0 and R_g at infinite time, it is most likely that the observed kinetics between pH 6.3 and 7.9 reflects the dissociation of the protein (48-mer) into two equal halves (24-mer), for which a sequential two-step reaction was suggested. On the other hand the kinetics above pH 8.0 indicated the dissociation into constituent subunits.

Keywords: Dissociation kinetics; *Limulus polyphemus* hemocyanin; Stopped-flow X-ray scattering

1. Introduction

Considerable evidence has been accumulated by means of ultracentrifugation and immunoelectron microscopy [1,2] that arthropodan hemocyanins are multimers of some fundamental submultiple which comprises six subunits. Four classes of the hemocyanins are known to occur in the arthropods in decreasing order of their

molecular mass, i.e. *Limulus polyphemus* (48-mer), *Androctonus australis* (24-mer), *Astacus leptodactylus* (12-mer) and *Panulirus interruptus* (hexamer).

In a previous paper from our group [3], a solution X-ray scattering (SXS) study was performed on hemocyanin from the horseshoe crab *L. polyphemus* and on its dissociated components obtained under a variety of conditions. Scattering patterns of native hemocyanin (48-mer), its half-molecules (24-mer), quarter-molecules (12-mer) and monomers, indicated that the radii of gyration for the four molecular species were 110.7, 91.3, 77.3 and 36.5 Å, respectively. The models

Correspondence to: Dr. K. Kimura, Division of Medical Electronics, Dokkyo University School of Medicine, Mibu, Tochigi 321-02, Japan.

constructed by eight, four and two spheres with a radius of 58 Å per sphere, fitted well with the experimental data.

Stopped-flow light scattering studies of the dissociation of *L. polyphemus* hemocyanin have been done by Brenowitz et al. [1] extensively. Recently, we developed a stopped-flow X-ray scattering (SFXS) method [4] and applied it to study the dissociation of aspartate transcarbamylase and phosphorylases [5–7]. It is the aim of this article to investigate the kinetic process of the dissociation of hemocyanin into low molecular components, by using the SFXS method. The results obtained will be discussed in relation to the dissociation mechanism, in comparison with the result obtained by Brenowitz et al. [1].

2. Materials and methods

Hemocyanin (48-mer) was purified from the hemolymph of the horseshoe crab (*L. polyphemus*) as previously described [3]. SFXS experiments were carried out at the beam-line 15A1 of the Photon Factory of the National Laboratory for High Energy Physics (Tsukuba, Japan). Details of the experimental procedure were reported elsewhere [3]. A stopped-flow apparatus specially fabricated for X-ray scattering was used in the experiment. Characteristics of the stopped-flow apparatus were described previously [8]. The dead-time of mixing was 10 ms. Minimal sample volume for one shot was 180 µl.

Data acquisition and data analyzing system were described elsewhere [3,9]. Data were mainly analyzed in terms of zero-angle intensity, I_0 (cps), radius of gyration, R_g (Å), and partially integrated scattering intensity, I_p . I_0 and R_g were obtained from the intercept of vertical axis at $h = 0$ and the slope of Guinier plots, respectively, where the angle argument is given as $h = 4\pi \sin \theta / \lambda$ (2θ = scattering angle, λ = wavelength) [10,11]. I_0 is known to be proportional to cM , where c is the protein concentration and M is the molecular weight, and R_g stands for the average size of the molecule [12]. By contrast, I_p is thought to reflect conformational states, such as subunit arrangements, in sharp sensitivity [13,14].

Dissociation experiments of hemocyanin were carried out by mixing a hemocyanin sample (9% w/v hemocyanin, 50 mM Tris-HCl, (ionic strength, $I = 0.15$), 10 mM CaCl_2) with dissociation buffer (50 mM Tris-HCl ($I = 0.15$), 28.5 mM EDTA) at a ratio of 1:3.5. pH of the sample solution and dissociation buffer were adjusted to the same prior to the reaction. Each measurement was done at 25°C.

Stopped-flow fluorescence experiments were performed with the UNISOKU USP-500 rapid reaction analyzer spectrophotometer at a mixing ratio of 1:1. The mixed solution was excited with the light of 280 nm, and the emission light having wavelengths longer than 310 nm was collected perpendicular to the incident light.

3. Results and discussion

3.1 Dissociation of hemocyanin (48-mer) into 24-mer

Figure 1 illustrates time-resolved change of the SFXS pattern from 48-mer to 24-mer dissociation induced by calcium removal on addition of EDTA at pH 7.0. In the figure scattering patterns obtained from the 1st, 25th and 95th frames are

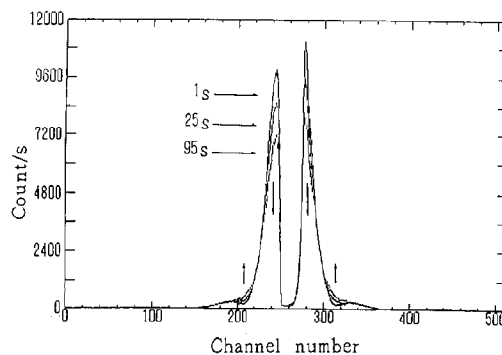


Fig. 1. Time-resolved X-ray scattering patterns of *L. polyphemus* hemocyanin sample after mixing with the dissociation buffer. One volume of the protein solution (hemocyanin, 9% w/v, pH 7.0, Tris-HCl, $I = 0.15$, 10 mM CaCl_2) was mixed with 3.5 volume of the dissociating reagent (pH 7.0, Tris-HCl, $I = 0.15$, 28.5 mM EDTA). Data were acquired at each 1 s/frame. Scattering patterns at the first, 25th and 95th frames are indicated by the numeral with arrow.

shown. They represent the patterns taken 1, 25 and 95 seconds, respectively, after mixing the hemocyanin sample with the dissociation buffer. The figure indicates that the patterns of the 1st and 95th frame were consistent with those obtained for the 48-mer and 24-mer in the static study [3] and that scattering intensity of the small-angle region ($h = 0.011 \text{ \AA}^{-1}$ (280 channel)) decreased remarkably, whereas the first minimum in the medium-angle region ($h = 0.031 \text{ \AA}^{-1}$ (312 ch)) increased significantly, giving two iso-scattering points at $h = 0.021 \text{ \AA}^{-1}$ (295 ch) and 0.049 \AA^{-1} (340 ch). Figure 2 demonstrates the time course of the dissociation monitored by partially integrated scattering intensity (I_p) of the two regions. One (I_{p1}) is integrated scattering counts between $h = 0.011 \text{ \AA}^{-1}$ (280 ch) and 0.018 \AA^{-1} (290 ch), and the other (I_{p2}) is those between $h = 0.024 \text{ \AA}^{-1}$ (300 ch) and 0.043 \AA^{-1} (330 ch). Total counts for the I_{p1} and I_{p2} were plotted as a function of time (Fig. 2).

Here two partially integrated parts were selected because: the small-angle region ($h = 0.011\text{--}0.018 \text{ \AA}^{-1}$) is an indicator of the change in radius of gyration, R_g , i.e. the overall size of protein, while the medium angle region ($h = 0.024\text{--}0.043 \text{ \AA}^{-1}$) provides information concern-

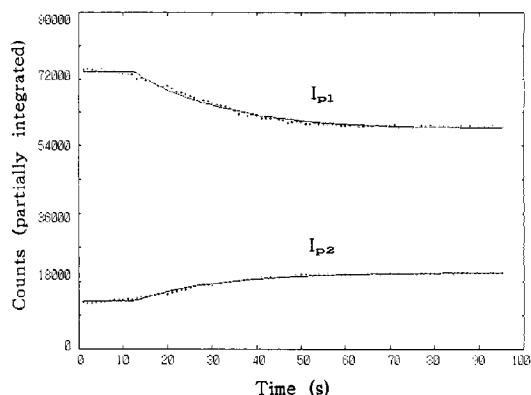


Fig. 2. Time course of partially integrated scattering counts of the hemocyanin dissociation. Scattering counts between $h = 0.011$ and 0.018 \AA^{-1} (I_{p1}), and between $h = 0.024$ and 0.043 \AA^{-1} (I_{p2}). Broken lines are simulated curves according to eq. (1). Experimental conditions are the same as in Fig. 1.

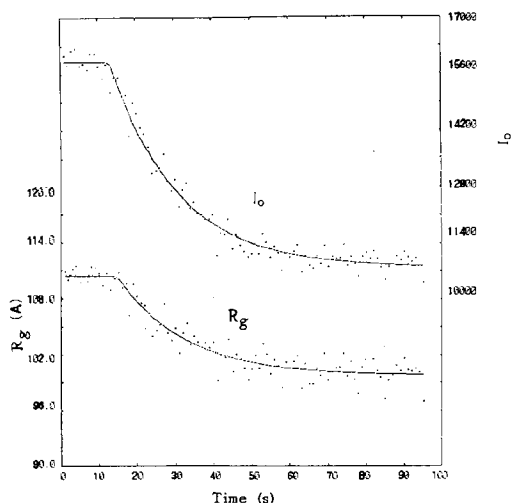


Fig. 3. Time course of the zero-angle intensity (I_0) and the radius of gyration (R_g) after mixing with EDTA at pH 7. Broken line shows a simulated curve according to either eqs. (2) or (3). Experimental conditions as in Fig. 1.

ing molecular conformation of protein [8,9,13]. As is seen in the figure, both curves demonstrate a time lag of about 13 s, followed by an exponential decrease or an increase in the I_{p1} and I_{p2} , respectively. The decrease in I_{p1} demonstrates that the native hemocyanin (48-mer) has dissociated into smaller components, while the increase in I_{p2} indicates that the molecular conformation of the protein has changed. The synchronism of the kinetic profiles of I_{p1} and I_{p2} suggests that either change took place at the same time.

Values of zero-angle intensity (I_0) and radius of gyration (R_g) were also estimated from the scattering patterns by Guinier plotting of data in each time frame as previously described [3], and then were plotted as a function of time, as shown in Fig. 3. An initial lag followed by a single exponential decay was observed for both curves.

A similar decay in the dissociation kinetics of hemocyanin was reported by Brenowitz et al., as monitored by light scattering [1]. They estimated the pseudo-first order rate constant (k') by using the data in the initial 10% of the reaction, regardless of its increase in the later part of the dissociation process. Considering the presence of a lag-

time, however, we attempted to calculate I_p , I_0 and R_g from the following equations.

$$I_p = I_{pf} + (I_{pi} - I_{pf}) e^{-k_{app}(t-t_d)} \quad (1)$$

$$I_0 = I_{of} + (I_{oi} - I_{of}) e^{-k_{app}(t-t_d)} \quad (2)$$

$$R_g = R_{gf} + (R_{gi} - R_{gf}) e^{-k_{app}(t-t_d)} \quad (3)$$

where t and t_d stand for the reaction time and lag time, respectively. The subscripts 'i' and 'f' denote 'initial' and 'final', respectively, and are defined as the values at $t = t_d$ and at $t = \infty$, respectively. The 'final' values were obtained for practical reasons from the data analysis with eqs (1)–(3) where t was extrapolated to infinity, which does not necessarily exclude the possibility that any other extremely slow process may be involved. As is evident from Figs. 2 and 3, curves (full lines) simulated from eqs. (1)–(3) for I_{p1} , I_{p2} , I_0 and R_g fit the data points well, thus supporting the validity of the equations. The apparent rate constant (k_{app}) and lag-time (t_d) were ob-

Table 1

Lag-times and k_{app} estimated for I_{p1} , I_{p2} , I_0 and R_g (For experimental conditions refer to the Fig. 1)

Parameter	Lag-time (s)	k_{app} (s ⁻¹)
I_{p1} (I_p between $h = 0.011$ and 0.018 \AA^{-1})	12.5	0.0472
I_{p2} (I_p between $h = 0.24$ and 0.043 \AA^{-1})	12.6	0.0498
I_0	12.7	0.0503
R_g	14.7	0.0466

tained from the data points of four parameters (I_{p1} , I_{p2} , I_0 and R_g). Results are summarized in Table 1. As seen in the table, the lag and k_{app} corresponding to the four parameters were in agreement with each other within experimental error. This fact suggests that the change in conformation of the molecule, associated with the dissociation, took place in a concerted manner.

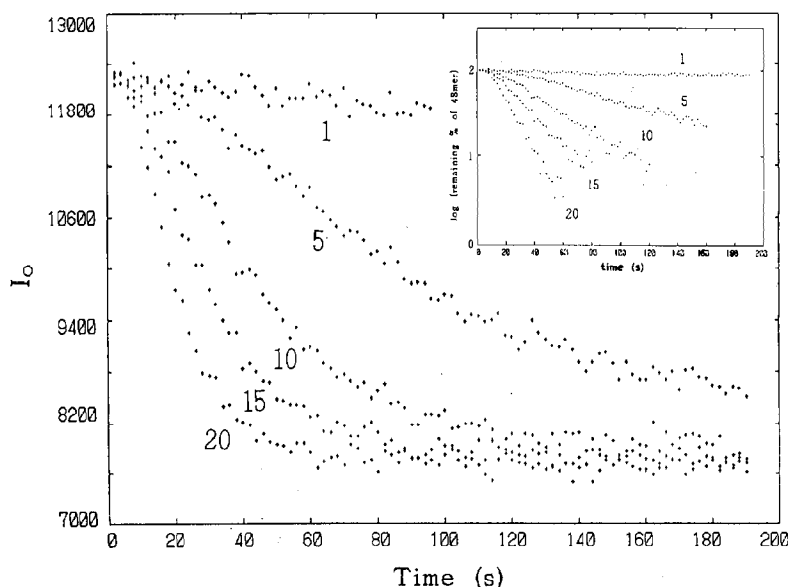


Fig. 4. Time course of the I_0 at various concentrations of uncomplexed EDTA. Uncomplexed EDTA concentration is the remaining portion of the chelator which is not complexed with calcium ions after mixing. The inset shows the first-order rate of reaction (dissociation) plot of the same experiment. Conditions are identical to those in Fig. 1, except for the chelator concentration which is indicated by the numerals (mM).

3.2 Factors affecting the dissociation

3.2.1 EDTA effect

The effect of EDTA concentration on the dissociation was studied. When the protein solution was mixed with EDTA in equimolar amount to free Ca^{2+} , no change was observed so far as measured (data not shown). This indicates that the presence of uncomplexed EDTA (ucEDTA), which represents the remaining portion of the chelator in solution that is not bound to free Ca^{2+} , is essential to the dissociation process. In other words, not only complete chelation of free Ca^{2+} but also further removal of Ca bound to the protein is required for dissociation to occur.

In Fig. 4, time courses of I_0 under various concentrations of ucEDTA are shown. The figure demonstrates that the kinetics became faster as concentration of ucEDTA increased, while the lag-time was shortened. In the presence of 1 mM ucEDTA, a very slow decrease in I_0 -value was noticed. The initial value of I_0 , which was 12,300 cps from the tangent to the initial part of the time course, agreed well with that obtained from the 48-mer in absence of EDTA (data not shown).

With increasing concentrations of ucEDTA, the I_0 -value decreased faster, while the lag-time was shortened as seen in the figure. As is evident from the figure, the I_0 -value reached a minimum of 7,700 cps, in the presence of 10–20 mM ucEDTA. This value coincided well with that obtained for the 24-mer, as described as previously reported [3]. The data were analyzed according to eqs. (2) and (3) to obtain each parameter. I_{0i} , obtained from the estimation, was $12,250 \pm 53$ cps, and I_{0f} was $7,770 \pm 65$ cps (the case of ucEDTA = 1 mM is excluded). The found agreement strongly supports the initial and final states are 48-mer and 24-mer for each ucEDTA concentration. By using $I_{0i} = 12,300$, and $I_{0f} = 7,700$, the data were plotted as a first order reaction (inset of Fig. 4). In concordance with the result of Fig. 4, the reaction proceeded linearly (i.e. first-order reaction) after the induction period. The slope obtained from the linear part of the reaction conformed well with the k_{app} -value calculated from eq. (2). The lag-time obtained from the point of intersection of the I_{0i} -value and the

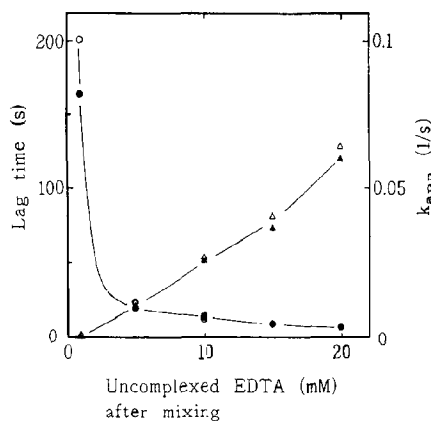


Fig. 5. Effect of uncomplexed EDTA concentration on the lag-time and k_{app} . Conditions are as for Fig. 1, except for EDTA concentration. Lag-time of I_0 (\circ) and R_g (\bullet), and k_{app} of I_0 (Δ) and R_g (\blacktriangle).

extrapolated linear part of the reaction was in good agreement with that calculated from eq. (2). A similar tendency was observed for the time course of R_g . These results also prove the validity of the equations.

Figure 5 summarizes the values of k_{app} and lag-time thus obtained from the time course of I_0 and R_g , for various concentrations of ucEDTA. It is to be noted that both I_0 and R_g values agree well with each other at the corresponding chelator concentration, indicating simultaneous occurrence of the change in size and shape of the protein. The increase of the k_{app} and decrease of the lag-time in either I_0 or R_g curve were remarkable with increasing ucEDTA. The steep increase of the lag-time with decreasing concentration of ucEDTA again clearly indicates that little dissociation occurs at zero concentration of ucEDTA. Brenowitz et al. reported that complete chelation of free Ca^{2+} in solution occurred within the dead-time (2.3 ms) of their rapid mixing apparatus and the chelation rate was instantaneous relative to the rate of the protein dissociation [1]. The lag-time obtained in the present study was in the order of seconds, much greater than the chelation rate of free Ca^{2+} in solution. This fact suggests that the lag-phase is the time required for the removal of a critical number of

Ca^{2+} from the 48-mer before dissociation takes place.

As may be seen in the same figure, the k_{app} -value approached to zero with decreasing ucEDTA, indicating also that no dissociation occurs in the absence of ucEDTA. In contrast to our results, Brenowitz et al. suggested that the 60 S hemocyanin (48-mer) dissociated to the 37 S component (24-mer) without facilitation of Ca removal from the protein on the basis of their experiment in which a pseudo-first order rate constant of $2.7 \times 10^{-3} \text{ s}^{-1}$ at zero chelator concentration was obtained by extrapolation. However, it is evident from the present investigation that ucEDTA is necessary to initiate the dissociation.

Based on these findings, the following two dissociation mechanisms are suggested:

(1) One kind of Ca-binding site is involved in the dissociation. Removal of Ca from the native 48-mer by the chelator leads to the formation of the decalcified 48-mer without change in neither I_0 nor R_g (Step I). The time required for this process is the lag. The decalcified 48-mer dissociates spontaneously into the 24-mer (Step II). The k_{app} estimated appears to depend on the chelator concentration, which can be ascribed for as a result of sequential reaction, i.e. the apparent chelator dependence of the k_{app} seems to be due to an increasing supply of the decalcified 48-mer which is produced chelator-dependently at the Step I.

(2) Two kinds of Ca-binding site play a role in the dissociation. In this model, removal of one Ca from the native 48-mer by the chelator forms an intermediate 48-mer without change in neither I_0 nor R_g (Step I). Removal of another Ca from the intermediate 48-mer by the chelator initiates dissociation (Step II). This model might explain the results that the lag and k_{app} both depend on chelator concentration.

A conclusive choice for one of the two alternative mechanisms must await further investigation especially for the process of Ca removal from the 48-mer (Step I).

3.2.2 Effect of pH

The dissociation kinetics of the hemocyanin was investigated at various pH values between 6.3

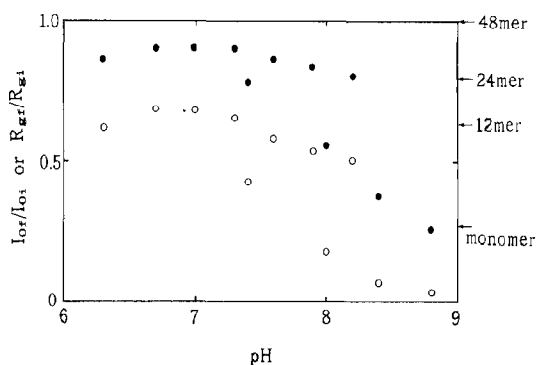


Fig. 6. pH dependence of the dissociation in terms of the ratio of I_{0f}/I_{0i} (\circ) and of R_{gf}/R_{gi} (\bullet). The indications at the right hand side are calculated by convention on the assumption that the molecules are spherical. R_g of 48-mer was selected as a standard. Conditions are as for Fig. 1, except for pH.

and 8.8. In this pH range except pH 8.8, time course of I_0 and R_g showed a lag followed by a single exponential decay as seen at pH 7.0. At pH 8.8, however, only a single exponential decay without a lag was observed. The ratio of I_{0f} to I_{0i} was calculated and plotted against pH in Fig. 6. As seen in the figure, the ratio of I_{0f}/I_{0i} (open circles) retained a fairly constant value of about 0.6 (av. 0.595 ± 0.258) below pH 8.0, whereas it decreased above pH 8.0 and reached 0.034 at pH 8.8. The average ratio of 0.6 below pH 8.0 is in agreement with that of I_0 (24-mer)/ I_0 (48-mer), viz. 0.56, obtained from the static experiments at pH 7.0 [3]. This fact supports that the protein dissociated into two halves (24-mer) by Ca removal between pH 6.3–8.0, in accordance with the ultracentrifugal analysis [1].

The ratio of 0.034 obtained at pH 8.8 suggests that the protein dissociated into monomers as the predominant species under this condition, as judged from the ultracentrifugal analysis [1] and our previous static study [3]. It was not possible to compare the ratio with the ratio of I_0 (monomer)/ I_0 (48-mer), since we failed to obtain it in the previous investigation [3]. Intermediate values of the ratio (I_{0f}/I_{0i}) observed at a pH range of 8.0–8.4 imply that the protein was probably resolved into a mixture of 24-mers and monomers.

A similar pH dependence of the ratio of R_{gf}/R_{gi} was shown in the same figure (closed circles). The arrows at the right hand side indicate calculated values of R_{gf}/R_{gi} for convention to represent the molecular assembly in the assumption that the molecules are spheres in the native hemocyanin and its dissociation product. It is evident from the figure that the hemocyanin dissociated into 24-mers at a pH range of 6.3–7.4 and into monomers at pH 8.8, in agreement with the result of I_{of}/I_{oi} .

As shown in Fig. 7, the k_{app} obtained from either I_0 or R_g , decreased with an increase of pH up to 7.4 and then reached a minimum above 7.4, although k_{app} for I_0 at pH 8.8 showed a higher value than the average of k_{app} between pH 7.6 and 8.4. These results indicate that the 48-mer to 24-mer dissociation occurs preferentially on the acidic side and decreased with increasing pH, where some ionizing groups may be involved in the dissociation at a pH range of 6.3–7.4. Further, the minimum attained above pH 7.4 implies termination of the 48-mer to 24-mer dissociation and switch over to another dissociation, possibly

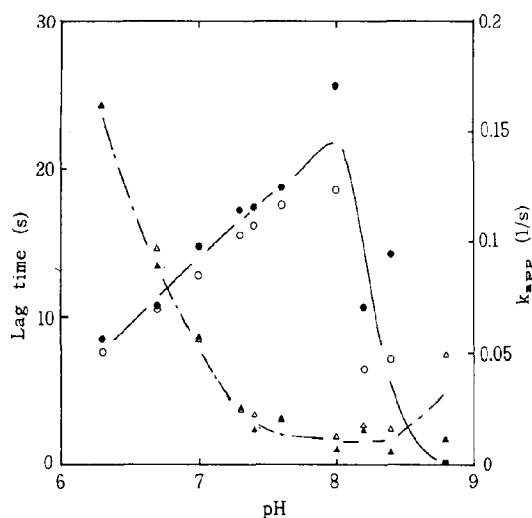


Fig. 7. pH dependence of the k_{app} and lag-time. Lag-time of I_0 (○) and R_g (●), and k_{app} of I_0 (△) and R_g (▲). Conditions are as for Fig. 1, except for pH.

to the monomer, in agreement with the result obtained from the final values of I_0 and R_g (see Fig. 6).

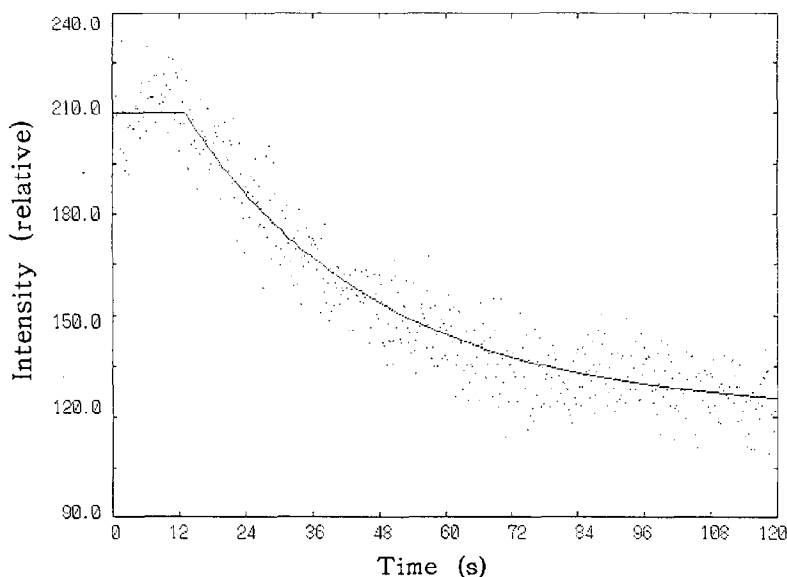


Fig. 8. Time course of the dissociation process of the hemocyanin as estimated by the fluorescence stopped-flow method. The protein solution (1%, 10 mM CaCl_2 , Tris-HCl, pH 7.0, $I = 0.15$) was mixed with the dissociation buffer (Tris-HCl, 20 mM EDTA, pH 7.0, $I = 0.15$). Final protein concentration was 0.5%. Full line represents a simulated curve by using the eq. (2), where I_0 was replaced by the relative fluorescence intensity.

Figure 7 also illustrates that the lag-time increased inversely to the k_{app} with increasing pH between 6.3–8.0. Elongation of the lag as well as the decrease of the k_{app} indicates suppression of the 48-mer to 24-mer dissociation, especially of the preliminary removal of the bound Ca from the 48-mer by EDTA at the Step I. Around pH 8.0 the lag attained to its maximum and then decreased above pH 8.0, reaching to zero at pH 8.8. This decrease of the lag also supports that another dissociation probably to the monomer occurs at this pH range as above described.

3.4 Dissociation monitored by fluorescence stopped-flow technique

The 48-mer to 24-mer dissociation process was also investigated by means of the fluorescence stopped-flow technique between pH 7.0 and 8.2. A typical time course of the fluorescence change after mixing the sample with the dissociation buffer at pH 7.0 is shown in Fig. 8, in which a lag and a subsequent single exponential decay were observed in a similar fashion to those of this SFXS study. The lag-time and k_{app} of the fluorescence decay estimated at varied pH were in good agreement with those obtained by the SFXS method. These results indicate some conformation change of the hemocyanin molecule associated with the dissociation, though give no direct information on the change of the molecular mass. Presence of the lag and sequential decay in the conformation change estimated by the fluorescence technique also supports the dissociation mechanism above mentioned.

Acknowledgments

We wish to thank Dr. Z.-X. Wang, Laboratory of Molecular Enzymology, Institute of Biophysics, Academia Sinica and Dr. Y. Amemiya, Photon Factory, National Laboratory for High Energy Physics, for helpful advice in this study. We are grateful to Dr. H. Sugita, Tsukuba University

who provided us with the hemolymph of *L. polyphemus*.

This work was supported in part by a Grant-in-Aid for Scientific Research (No. 03680232) from the Ministry of Education, Science and Culture of Japan and has been performed under the approval of the Photon Factory Program Advisory Committee (Proposal No. 85-151 and 88-060).

References

- 1 M. Brenowitz, C. Bonaventura and J. Bonaventura, *Biochemistry* 23 (1984) 879.
- 2 J.N. Lamy, J. Lamy, P. Billiald, P.-Y. Sizaret, J.C. Taveau, N. Boisset, J. Frank and G. Motta, in: *Invertebrate oxygen carriers*, ed. B. Linzen (Springer-Verlag, Berlin, 1986) p. 185.
- 3 K. Kimura, Y. Igarashi, A. Kajita, Z.-X. Wang, H. Tsuruta, Y. Amemiya and H. Kihara, *Biophys. Chem.* 38 (1990) 23.
- 4 Z.-X. Wang, H. Tsuruta, Y. Honda, Y. Tachi-iri, K. Wakabayashi, Y. Amemiya and H. Kihara, *Biophys. Chem.* 33 (1989) 153.
- 5 H. Kihara, T. Furuno, A. Ikegami and M.H.J. Koch, *Biochemistry (Life Sci. Adv.)* 6 (1987) 211.
- 6 H. Kihara, E. Takahashi-Ushijima, Y. Amemiya, Y. Honda, P. Vachette, P. Tauc, T.E. Barman, P.T. Jones and M.F. Moody, *J. Mol. Biol.* 198 (1987) 745.
- 7 H. Tsuruta, T. Sano, P. Vachette, P. Tauc, M.F. Moody, K. Wakabayashi, Y. Amemiya, K. Kimura and H. Kihara, *FEBS Lett.* 263 (1990) 66.
- 8 H. Tsuruta, T. Nagamura, K. Kimura, Y. Igarashi, A. Kajita, Z.-X. Wang, K. Wakabayashi, Y. Amemiya and H. Kihara, *Rev. Sci. Instrum.* 60 (1989) 2356.
- 9 Y. Amemiya, K. Wakabayashi, T. Hamanaka, T. Wakabayashi, T. Matsushita and H. Hashizume, *Nucl. Instrum. Methods* 208 (1983) 471.
- 10 A. Guinier and G. Fournet, in: *Small-angle scattering of X-rays* (Wiley New York, NY, 1955).
- 11 I. Pilz, in: *Small angle X-ray scattering*, eds. O. Glatter and O. Kratky (Academic Press, London, 1982) p. 239.
- 12 H. Pessen, T.F. Kumosinski and S.N. Timasheff, in: *Methods in enzymology*, ed. C.H.W. Hirs and S.N. Timasheff, Vol. XXVII (Academic Press, London, 1973) p. 151.
- 13 M.F. Moody, P. Vachette and A.M. Foote, *J. Mol. Biol.* 133 (1979) 517.
- 14 T. Ueki, Y. Hiragi, M. Kataoka, Y. Inoko, Y. Amemiya, Y. Izumi, H. Tagawa and Y. Muroga, *Biophys. Chem.* 23 (1985) 115.